The 2009 L'Aquila (Central Italy) Seismic Sequence.

L. Chiaraluce[1], C. Chiarabba[1], P. De Gori[1], R. Di Stefano[1], L. Improta[2], D. Piccinini[2], A. Schlagenhauf[3], P. Traversa[3], L. Valoroso[1] and C. Voisin[3].

[1] Centro Nazionale Terremoti, Istituto Nazionale di Geofisica e Vulcanologia. Via di Vigna Murata, 605 – Rome (Italy).

[2] Sezione Roma1, Istituto Nazionale di Geofisica e Vulcanologia. Via di Vigna Murata, 605 – Rome (Italy).

[3] Laboratoire de Géophysique Interne et Tectonophysique, Grenoble (France).

In press on Bollettino di Geofisica Teorica e Applicata.

Abstract.

On April 6 (01:32 UTC) 2009 a M_W 6.1 normal faulting earthquake struck the axial area of the Abruzzo region in Central Italy. The earthquake heavily damaged the city of L'Aquila and its surroundings, causing 308 casualties, 70,000 evacuees and incalculable losses to the cultural heritage.

We present the geometry of the fault system composed by two main normal fault planes, reconstructed by means of seismicity distribution: almost 3000 events with $M_L \geq 1.9$ occurred in the area during the 2009. The events have been located with a 1D velocity model we computed for the area by using data of the seismic sequence.

The mainshock, located at around 9.3 km of depth beneath the town of L'Aquila, activated a 50° (+/- 3) SW-dipping and ~135° NW-trending normal fault with a length of about 16 km. The aftershocks activated the whole 10 km of the upper crust up to the surface. The geometry of the fault is coherent with the mapped San Demetrio-Paganica and Mt. Stabiata normal faults.

The whole normal fault system that reached about 50 km of length by the end of December in the NW-trending direction, was activated within the first few days of the sequence when most of the energetic events occurred.

The main shock fault plane was activated by a foreshock sequence culminated with a M_W 4.0 on the 30th of March (13:38 UTC), showing extensional kinematic with a minor left lateral component. The second major structure, located to the north close to Campotosto village, is controlled by a M_W 5.0 which occurred on the same day of the main shock (the 6th of April at 23:15 UTC) and by a M_W 5.2 event (9th of April - 00:53 UTC). The fault plane shows a shallower dip angle with respect to the main fault plane, of about 35° with a tendency to flattening towards the deepest portion. Due to the lack of seismicity above 5 km depth, the connection between this structure and the mapped Monti della Laga fault is not straightforward. This northern segment is recognisable for about 12-14 km of length, always NW-trending and forming a right lateral step with the main fault plane. The result is a en-echelon system overlapping for about 6 km.

Seismicity pattern also highlights the activation of numerous minor normal fault segments within the whole fault system. The deepest is located at around 13-15 km of depth, south of the L'Aquila mainshock, and it seems to be antithetic to the main fault plane.

Introduction: the Seismotectonic Context.

During Quaternary, the region of the Central Apennines hit by the 2009 M_W 6.1 L'Aquila event (Figure 1), was deformed by active extensional tectonics following the eastward migration of the Apenninic compressional front. The result is a broad and complex system of normal faults developed in areas previously affected by compression (Galadini and Galli, 2000 and references therein).

In this portion of the chain extension occurs on an 50 km wide area (Selvaggi et al., 1997) that is accommodated, at least, on two major sub-parallel NW–SE trending normal fault systems (Vezzani and Ghisetti, 1998; Barchi et al., 2000; Galadini and Galli, 2000; Roberts and Michetti, 2004), unlike the contiguous Northern and Southern Apennines. The activity of these two systems produced large intermountain extensional basins such as L'Aquila, Sulmona and Fucino basins, filled by Plio- Quaternary continental sediments (Cavinato and De Cellis, 1999; Galadini and Galli, 2000). During the Quaternary, the normal and normal–oblique faulting was synchronous to a regional uplift (e.g. D'Agostino et al., 2001; Galadini and Galli, 2003) and the NE-trending extension is considered continuously active at least since the Early Pleistocene. The current rate of extension is 2–3 mm/year (Hunstad et al., 2003) and its orientation is consistent with available focal mechanism solutions (Montone et al., 2004), borehole break-out (Mariucci et al., 1999) and geological data (Lavecchia et al., 1994). Field geology based studies revealed the location and geometry of major faults. Some of them are thought to be responsible for large historical earthquakes that occurred in the region with M=7 such as the Fucino fault system associated to the 1915 Ms=7.0 earthquake (Figure 1; e.g. Ward and Valensise, 1989).

The closest and largest damaging historical earthquakes that struck the region occurred in 1461 close to the city of L'Aquila (I_{max}=X), and in 1703 slightly to the north (I_{max}=XI; CPTI Working Group, 1999). The location and geometry of the seismogenic sources of these events are not yet constrained, so we decided to show in Figure 1 both the macro-seismic epicentre and the locations (colour coded points) that for each event recorded the largest intensity. Some authors (e.g. Atzori et al., 2009, among others) suggest that the 1461 event may have occurred on the Paganica-San Demetrio segment (SDP; mapped by Bagnaia et al. 1992) responsible for the 2009 mainshock. However, despite dense temporary seismic surveys carried out in the area, the geometry at depth of the larger faults mapped as active are still unconstrained (Bagh et al., 2007) because background seismicity in the inter-seismic period appears sparsely distributed without evidencing clear fault planes (Chiaraluce et al., 2009).

In Figure 1 we also report the larger instrumental seismic sequences occurred in the region together with the location and focal mechanisms of the related main events.

From north-west to south-east, the Colfiorito (Chiaraluce et al., 2003) and Norcia (Deschamps et al., 1984) sequences occurred in 1997 and 1979, respectively. Both sequences activated SW-dipping normal faults. South-eastward we report the seismicity of the 2009 L'Aquila

sequence with its main shock location and dip-slip focal mechanism solution (Scognamiglio et al., in press).

During the past 20 years the area has only been affected by minor seismic episodes (in 1992, 1994 and 1996), while the background seismicity is sparsely distributed (Bagh et al., 2007 and Chiaraluce et al., 2009). Minor sequences are located close to the L'Aquila area, with a maximum magnitude M_L=4.0 (De Luca et al., 2000; Pace et al., 2002; Boncio et al., 2004; and Ciaccio et al., 2009).

In this study, we present a seismicity pattern for the whole year of 2009 in the source region of the L'Aquila earthquake. Then we use hypocentral locations obtained by using a 1D gradient P-wave velocity model and V_P/V_S ratios, computed for the area, to show the first order geometry of the activated normal fault system. The earthquakes have been recorded by the permanent Stations of the National Seismic Network (RSNC) managed by the Istituto Nazionale di Geofisica e Vulcanologia (INGV) until the 6th of April, and then by stations of the INGV temporary network, available a few hours after the L'Aquila mainshock. For two months after April we also benefited by data from an additional temporary network installed by the Laboratoire de Géophysique Interne et Tectonophysique (LGIT) of Grenoble. We use seismicity distribution and focal mechanisms of the major events to describe the geometry and kinematics of the activated fault system.

Earthquakes' Location and Seismic Catalogue.

Velocity model and V_P/V_S

We show in Figure 2A the two P-wave 1D velocity models available for the area together with the gradient velocity model used. The model by Bagh et al. (2007) (black line, model A) was computed with the Genetic Algorithms technique for a larger area including the study region. The model by Chiarabba et al., (2009) (grey line, model B) was computed with preliminary data of the L'Aquila sequence by inverting P- and S-wave arrival times with the VELEST code (Kissling et al., 1994). Both A and B velocity models are prone to the introduction of artefacts, namely horizontal earthquake alignments along discontinuities, due to the use of a layer-cake model. Such artefacts are more likely to be present when trying to represent a 3D complex structure with a 1D velocity model, while they disappear in 3D earthquake locations (Di Stefano et al., submitted). To choose the best reference 1D velocity model for our dataset we performed several preliminary earthquake location tests, trying to avoid artificial alignments of seismicity. Based on our results we ended up with the idea that a 1D layered cake model is in this case not adequate to be used for accurate 1D earthquake locations due the very complex 3D structure of the L'Aquila region. Thus we prefer to use a smooth-gradient model (red line in Figure 2A) showing P-wave velocity values very close to those of models A and B, but continuously defined top to bottom. Lower P-wave velocities at the surface, with respect to the other two models, are compatible with the presence of low velocity sedimentary units

outcropping in the epicentral area and in the northern sector of the fault system (Capotosto area). The gradient velocity model used in this study consists of a V_P velocity that increases linearly from V_0 (5.0 km/s) at the surface by 0.15 km/s per kilometre until the half space is reached at a depth of 10 km. The velocity within the half space is 6.51 km/s.

The mean V_P/V_S ratio was determined by using a cumulative Wadati diagram. Lucente et al. (2009) and Di Luccio et al. (2010) observed that the ratio changed with time during the sequence and mainly before and after the mainshock occurrence. In agreement with these studies we decided to compute and use one value for the foreshocks (1.86) and a different one for the aftershocks (1.90). The Wadati diagrams showed in Figure 2B and 2C illustrate the robustness of these measurements.

Parameters Setting and Data Weighting in the Location Procedure

A few hours after the main shock numerous temporary stations were installed both in the epicentral area and at the edge of the fault system, with a double aim: to reduce the average spacing from stations from about 15 km (of INGV permanent network) to 7-8 km and to be able to follow the possible migration of seismicity. This emergency intervention allowed us to obtain very high quality location throughout the seismic sequence evolution. We compute earthquakes location with the Hypoellipse code (Lahr, 1989) setting parameters differently for different time intervals modulated on the network geometry evolution. Luckily, this prompt expansion and improvement of the network density and geometry, allowed us to follow the expansion of the epicentral area due to the activation of secondary structures after the mainshock occurrence. We divided the whole period in 5 different time windows in reason of the mean distance between the available seismic stations (see Table 1): 1) the stations of the RSNC (grey squares in Figure 3) with mean distance of 30km (from the 1st of January to the 12:00 p.m. of the 6th of April); 2) RSNC plus the first 8 stations of the INGV mobile network installed a couple of hours after the mainshock occurrence. The mean distance is 20km (from the 12:00 pm of the 6th of April to the 7th of April); 3) RSNC plus all of the 20 INGV mobile network stations (grey triangles in Figure 3) installed with a maximum distance of about 15 km (from the 7th to the 9th of April); all the local and permanent INGV stations plus other 20 stations of the LGIT mobile network (grey diamonds in Figure 4) that further reduced the spacing below 10km (from the 9th of April to the 26th of June). 5) The last period, going from the end of June to the end of 2009, has the same configuration as the third one.

Table 1. Networks available in 2009 for the Abruzzo region. See the text for the details of the installation timing of the temporary stations during the first hours-days after the main shock occurrence. PN: permanent network; MN: mobile network.

J	F	M	A	M	J	J	A	S	O	N	D	Month
x	x	x	x	x	x	X	x	x	x	x	X	RSNC-PN
			x	x	x	X	x	x	x	x	X	Ingv-MN
			x	x	x							Lgit-MN

In the location procedure we changed the weighting scheme with distance and the azimuthal coverage, accordingly to the network evolution. We also used the elevation correction option using the first layer velocity up to a mean topography of 500 m that we derived computing the mean altitude of the stations position.

Foreshocks and Aftershocks Catalogues

We compiled the foreshock and aftershock catalogues by applying two different sets of selection parameters, based on the different network geometries illustrated above.

For the foreshocks that we define here as the events occurred in the study region from the 1st of January to the 6th of April at 1:30 a.m. UTC, only data recorded at stations of the RSNC are available. Due to the lower number of available stations, we decided to reprocess the data directly from the continuous recordings of all the stations located within 100 km from the mainshock, by using a more sensible triggering algorithm with the aim to detect a larger number of smaller magnitude earthquakes. The triggering algorithm individuated 2861 coincidences at a minimum number of three stations. Then, we ran our automatic picking code on these data (MPX; Aldersons et al., 2009) for P- and S-waves. We end up with 1716 locatable events that after the first location process shows the resolution parameters showed in Figure 4. From these data we selected a final subset of 561 well located events with a final rms < 0.4 s, azimuthal gap minor of 200°, a minimum number of 4 arrival times and horizontal/vertical (ERH-Z) formal errors < 1.5 km.

For the aftershocks (from the 6th of April - 01:32 UTC to the end of 2009), we selected all the events with $M_L \geq 1.9$ from the whole catalogue of 18867 events recorded and located within the epicentral area by personnel on duty 24 hours a day at the INGV National Earthquake Centre. No triggering algorithm was applied. We simply cut waveforms 50s and 120s before and after the origin time of the event respectively. Then we run the MPX on each earthquake. From the starting 3044 events (location parameters are reported in Figure 5), we end up with 2643 events with rms < 0.2 s, ERH-Z < 1km, gap < 200°and more than 8 P- and 4 S-readings.

The very high quality of the recovered absolute hypocentral locations for both datasets mainly derives from the exceptional performance of the automatic picker that has its main strength in the homogeneity of data weighting (Aldersons et al., 2009).

Seismicity Pattern.

In the spatio temporal evolution diagram (Figure 6) we observe that the seismicity before and after the occurrence of the foreshock (30th of March at 13:38; M_W 4.0) generally took place in the epicentral area. Soon after the mainshock (6th of April at 01:32 UTC; M_W 6.1) seismicity started to spread migrating from the central area identified as the town of L'Aquila toward the Campotosto village, located to the north-west. Here the other main fault segment was activated within the first couple of days, as indicated by a M_W 5.0 event occurred on the same day of the main shock (the 6th of April at 23:15 UTC) and by a M_W 5.2 event on 9th of April (at 00:53 UTC). In general, the larger amount of energy was released within the first week of aftershocks by events located on these two main fault planes. In the following three months, minor events mostly occurred within the whole main system, until the end of June when seismicity started to cluster around the Cittareale area located around 10 km further to the north-west (Figure 1). Though the larger event of this latter cluster is a M_W 3.5 (25th of June - 21:00 UTC), the seismicity rate in this small area was high enough to be clearly visible on the curve showing the cumulative number of events for the whole period (Figure 7). Also the activation of the flat and deepest portion of the Campotosto segment, occurred at the end of June with a main event of M_W 4.4 (22nd of June - 20:58 UTC; brown star in section 9 of Figure 10) contributed to this acceleration in the seismic release.

The majority of earthquakes in terms of cumulative number of events versus time, occurred in the week after the mainshock (black star in Figure 7), and for the first three months after we detect a Omori like decay: a rapid increase in the rate of production followed by an abrupt (e.g. inverse power) decay with time (Omori, 1895).

The distribution of the seismicity versus depth (Figure 8) shows that the majority of the events occurred between 2 and 9 km of depth, but we also observe a deeper break around 15 km. This characteristic of the Abruzzi region is in agreement with Bagh et al. (2007) and it seems to confirm that in this portion of the Central Apennine the width of the active seismogenic volume is at least 4 km thicker than in the Northern Apennine. Figure 8 also shows that the foreshocks (red line) do not generally occur shallower than 5 km; however, the majority of large events (purple line) nucleate between 6 and 10 km of depth. Only one large event, with M_W 5.4 occurred around 14 km depth (7th of April, 17:47 UTC).

By the end of December the maximum length of the fault system imaged by earthquake distribution is in the order of 50 km along the N45°W-trending direction (Figure 6).

Fault System Geometry.

In this paragraph we use seismicity distribution to reconstruct the geometry of the normal fault system activated during the seismic sequence. Hypocentral locations of the 561 foreshocks (red points) and 2643 aftershocks (black points) appear in map view in Figure 9

and in a set of vertical cross sections in Figure 10. In the map view we also report the mapped active faults of the area (brown lines in Figure 9) and the ~5 km of surface breaks mapped by the EMERGEO Working Group (2010) the days soon after the mainshock occurrence (yellow line). The cross sections have been drawn perpendicular to the average strike of the main structures (NE45°; Anzidei et al., 2009; Atzori et al., 2009). Sections width are symmetrical (northwest-southeast) perpendicularly to the trace but the width of each section is different to better describe the geometry of the specific portion and sections edges never overlap. In map and sections stars depict all the events with M_W>3.5, with dimension and colour code based on the magnitude. For these events, M_W has been obtained by Scognamiglio et al. (in press) by using the time domain moment tensor technique.

The Southern Area.

This area is delimited to the north by the presence of the largest and deepest event of the sequence: a M_W 5.4, occurred the 7th of April at 17:47 UTC at 14.1 km of depth (blue star in section 3 of Figure 10; see location in map in Figure 9). This event is characterised by a small number of aftershocks occurring in the first couple of days (of what?). The focal mechanism (Figure 11) shows a normal faulting solution with a minor strike slip component. Based on the distribution of the few aftershocks, we select the ENE-dipping plane at high angle (~60°) in between the two of the nodal planes for this event, denoting a left lateral component in the dip slip kinematics. This deep and small segment, less than 4 km long, is antithetic to the main SW-dipping L'Aquila fault plane.

The shallower seismicity shows some minor alignments but not a clear geometry of a main fault plane. To better understand the geometry and the role of these minor segments we superimposed the seismicity contained in one section that well image the main L'Aquila plane (yellow points) to the first three cross sections of Figure 10. This portion of the system is missing a clear major plane but some events in section 3 seem to delineate few minor fault segments synthetic to the main system (sections 6, 11 and 12). Southward (sections 1 and 2) we observe the presence of a main cluster showing no specific alignment. The main remark here is that all these structures are located in the main fault hanging-wall. The absence of the main fault plane south of section 3 is in agreement with the L'Aquila 2009 fault model proposed by Anzidei et al. (2009) obtained by modelling the horizontal and vertical coseismic surface displacements observed at a set of 5 GPS stations. We report in Figure 9 the location of the southernmost GPS station named CADO located about 16 km south of the mainshock along strike, whose coseismic displacement signs the end of the main fault plane. We acknowledge that this area needs to be investigated possibly with higher resolution locations.

L'Aquila Area.

In this area, seismicity distribution clearly image the main fault plane of the system (sections 4-8 of Figure 10): a 50° (+/- 3) SW-dipping plane striking at about N135, activated by the mainshock of the 6th of April at 01:32 UTC with M_W 6.1 (blue star in section 6). The mainshock nucleated at ~9.3 km of depth at the base of the seismicity and shows a focal mechanism in perfect agreement with the geometry of the fault. Seismicity distribution clearly images the fault plane for at least 16 km of length activating all the first 10 km of the upper crust up to the surface where field geologists recognised co-seismic breakages for a length of about 5 km (EMERGEO Working Group, 2010). The location of these ruptures located along the SDP fault agrees with the seismicity termination towards the surface (sections 4, 5 and 6), though splitting of the main fault plane towards the end of the mapped SDP fault is observed where it encounters the Mt. Stabiata fault (MS). This segment forms a right lateral step with the SDP located more to the east (see fault traces in Figure 9). Here the shallower seismicity seems to flatten toward its intersection with the topography. Boncio et al. (2010) observed minor signature of surface ruptures also along ~3 km of the Stabiata fault and their interpretation is that a small amount of slip approached the surface co-seismically. Towards the surface seismicity images minor synthetic splays while in the deepest portions we observe quite large anti- and synthetic faults. Seismicity deeper than 10 km is present also in this area with a small sequence following a M_W 4.2 event occurred on the 9th of April (03:14 UTC) that delineates a high angle plane antithetic to the main fault and practically located in its foot-wall (section 4). The kinematics of this earthquake illustrated by the focal mechanism is very similar with the one showed by the deepest mainshock located in the southern area and described in the previous paragraph.

In sections 7 and 8 we observe many sub-parallel normal faults. In the main fault footwall we see the southern tip of the Campotosto fault (CMP), located to the east. This means that the Campotosto fault forms an en-echelon structure overlapped for almost 6 km, with the MS and SDP system. In between these two systems we note the presence of another minor sub-parallel segment. The activation of many structures in the main fault footwall is a characteristic of the L'Aquila 2009 system that we did not observe in the 1997 Colfiorito normal fault system (Chiaraluce et al., 2003).

Foreshock activity is confined in this area and this is the reason why we draw additional thinner cross sections. Looking at the foreshock sequence in map view of Figure 9 (red points) we observe a NW-trending elongated seismicity distribution, consistent with the L'Aquila fault plane related seismicity, and, to the south, an almost NS branch. Valoroso et al. (2009) observed that the sparser seismicity occurred before the foreshock generally nucleated around the main fault plane, whereas after the M_W 4.0 occurred on the 30th of April at 13:38 UTC (larger red star in section 5 of Figure 10), seismicity started to activate a minor segment almost antithetic to the main fault plane. Accordingly, the focal mechanism of the M_W 4.0 event shows a high angle E-dipping plane striking N-S with a left lateral component. Then, on the 5th of April, seismicity nucleation moved back to the main fault plane with the occurrence of two events felt by the population (20:48 UTC M_W 3.88 and 22:39 UTC with M_W 3.50; red stars in section 20).

Campotosto Area.

The SW-dipping Campotosto fault (sections 9-12) shows some notable differences with respect to the MS-SDP one. The fault plane is about 12-14 km long, somewhat smaller than the MS-SDP. In addition, the dip of the fault changes with depth. We discriminate the portion between 8 and 11 km of depth that dips about 35° from the shallower termination that dips steeper (about ~50°) up to 6 km of depth. On the contrary the deepest part of this complex fault segment shows a tendency to flattening. Focal mechanism solutions are in agreement with these observations. Moreover the higher magnitude events (M_W>4.5) nucleate exactly where the fault plane changes its dip showing a segmented shape rather than a clear listric profile (sections 9 and 10 in Figure 10).

Cittareale Area.

A small event with M_W 3.5, occurred on the 25th of June at 21:00 UTC (green star in section 13 of Figure 10), started the occurrence of a cluster of seismicity near the village of Cittareale located at about 8-10 km to the north-west of the main fault system. Although this small event is the largest occurred in this northernmost area, we observed a clear acceleration in the seismic release soon after its occurrence (Figure 7). Many small events occurred within a couple of months, with the M_W 3.5 event nucleating at the base of this cluster at 8 km of depth, but their spatial distribution does not allow to identify any fault geometry. Only in the last section drowned to the north (section 14) we can distinguish a possible alignment of seismicity. Antonioli et al. (2009) modelled the seismicity pattern of this sector and their preliminary results suggest that the spatio-temporal distribution of the seismicity is consistent with a pore-fluid pressure diffusion process.

Discussion and Conclusion.

We used seismicity distribution of the 2009 L'Aquila sequence to reconstruct the geometry of the activated normal fault system. We image two main fault segments: the San Demetrio-Paganica-Mt. Stabiata main fault and a second structure in the Campotosto area. The system is composed by SW-dipping planes, as previously proposed by geodetic data (Atzori et al., 2009; Walters at al., 2009). The main shock nucleated at the base of the larger SDP-MS segment is located exactly beneath the ancient city of L'Aquila (Chiarabba et al., 2009). The main shock position, together with source directivity (Cirella et al., 2009, Pino and Di Luccio, 2009 and Ellsworth and Chiaraluce, 2009) and site effects, contributed to the damage (Çelebi et al., 2010).

The larger SDP-MS segment (16-18 km of length) is a SW-dipping almost planar plane cross-cutting at high angle (50° +/-3) the all whole upper crust down to 10 km of depth. On the contrary, the smallest CMP fault (12-14 km of length) activated between 5 and 12 km of depth, shows a smaller dip (about 35°) and a segmented geometry along the fault width with a tendency to flattening towards the deepest portion. The major events (6 with M_W>4.5) that nucleated along this structure are located where the fault changes its dip and the focal mechanism solutions are in agreement with this observation.

The dip showed by the shallower seismicity located along the SDP-MS fault seems to be in agreement with the hypothesis of coseismic ruptures reaching the surface during the main slipping episode, as proposed by many Authors basing on geodetic (Anzidei et al., 2009; Atzori et al., 2009; Walters et al., 2009) and field geology studies (EMERGEO Working Group, 2010; Falcucci et al., 2009, Boncio et al., 2010). The innovative application of laser scan technology to survey after-slip seems to corroborate the hypothesis that a small amount of slip reached the surface (Wilkinson et al., 2009).

Conversely the CMP segment is completely blind and the overall relationship between the mapped geological structure named Monti della Laga fault and the CMP seismological fault (in the sense of Chiaraluce et al., 2005) is not straightforward due to the lack of seismicity in the first 5 km of the crust. Moreover, a further changing in the dip towards the surface would be needed to align the Campotosto seismicity with the geological fault trace at its intersection with the surface. Chiarabba et al. (2009) indicated this portion of the fault not interested by seismicity (an area of about 4 km by 10 km) as the possible location for a future moderate event. Antonioli et al. (2009) investigated this aspect by analysing static stress transfers and their preliminary results show that seismicity occurred on the deepest portion of the plane may have downloaded the (positive) stress in the upper termination of the fault.

Another important distinction in between the Campotosto and L'Aquila region is the presence in the crustal volume of several secondary structures. They are almost absent in the CMP area while they characterise both the L'Aquila fault hanging- and foot-wall. We ascribe the different pattern of strain release to significant differences in the crustal structure and lithology between the L'Aquila and Campotosto areas.

The upper crust in the mainshock area consists of a complex stack of shelf and slope carbonate units (Latium-Abruzzi platform, Triassic-Palaeogene). These deeply fractured units over thrust Mio-Pliocene flysch deposits along the northern (Laga Flysch) and the eastern (Queglia Unit) margins of the Gran Sasso thrust system (Calamita et al., 2004). Deep exploration data are not available in the Gran Sasso region, but the CROP11 seismic profile located about 20 km to the south of the epicentral area indicates that the stack of carbonate thrust sheets is up to 8 km thick (Patacca et al., 2008). Whilst the Campotosto area, located to the north of the Gran Sasso thrust system, is characterized by NNW-SSE trending fault-propagation folds, involving Triassic-Miocene sedimentary succession of the Umbria-Marche basinal domain (Mazzoli et al., 2005). In the hanging-wall of the Mt. della Laga fault, two deep

exploration wells (UNMIG Well Database, 2009) have penetrated a ~2 km thick plastic sequence (Laga Flysch, Cerrogna Marl and underlying Bisciaro Fm., lower-upper Miocene) overlying the typical carbonatic multilayer and evaporites of the Umbria-Marche stratigraphic sequence (Triassic-Oligocene). Consequently, brittle limestones characterize the mainshock region, whereas thick plastic Miocene sedimentary successions characterize the Umbria-Marche succession in the Campotosto area. Our speculation is that the latter northern volume may account for a larger component of aseismic deformation.

Moderate and large earthquake sequences in Central and Northern Apennines (Italy) typically activate NW-striking normal fault systems accommodating the extensional stretching of the belt. These systems are usually composed by adjacent and en-echelon (sopra era scritto con trattino) segments usually activated in a relatively short time span. The 2009 L'Aquila seismic sequence showing the activation of a normal fault system through main episodes of seismic ruptures delayed hours to days between them is tuned on this general observation. A complex mechanism of multiple failures on adjacent segments is observed both in recent instrumental and historic events (e.g. the 1997 Umbria-Marche sequence and the 1703 Norcia-Cascia earthquakes). For these events the time lapse between major events activating portions of the same system is in the order of hours or months. Fluids in the upper crust are often invoked to be the driving factor for this domino-like behaviour of multiple shocks, as well as for the migration of seismicity along adjacent faults. During the L'Aquila sequence we observe only a minor episode of seismicity migration occurring during the first two days after the main shock, when seismicity moved to the north-western portion of the system from L'Aquila to Campotosto (Figure 6). However, the rate of seismic release of the whole sequence can be easily modelled as a Omori like decay of the seismicity production giving evidence that the seismicity pattern behaves as a standard mainshock-aftershock seismic sequence (Omori, 1895). We believe that these findings have to be taken into account when interpreting the observed variations in the V_P/V_S with time. Lucente et al. (2009) interpreted the variation of the Poisson ratio observed during the foreshock sequence as an example of dilatancy process that contributed to decrease the normal stress on the main fault plane. While Di Luccio et al. (2010) proposed that a pore fluid pressure diffusion process may control the whole space-time evolution of aftershocks sequence.

Finally, as observed for the majority of the larger instrumental events occurred in Italy in the past 20 years, surface evidences of the fault dislocation of the L'Aquila earthquake are tiny, making it difficult to interpret. This aspect amplifies our challenge in precisely locating the segments driving the larger deformation episodes of this portion of the Apennines, as testifiedby the absence of the San Demetrio-Paganica fault in the consensus catalogue of the active faults of the area (Barchi et al., 2000).

At the same time we believe that the extraordinary data collected for the L'Aquila sequence by multidisciplinary geophysical networks will allow us a better modelling and interpretation of the deformation style of the area for the future improvement of earthquake hazard models.

Figure Captions.

Figure 1: Map view (a) and (b) longitudinal cross section of the historical (CPTI, 1999), instrumental seismicity plus focal mechanisms of the largest events (Chiaraluce et al., 2007 and reference therein; Scognamiglio et al., in press). Large circles (in map) represent the location of the largest intensities for each historical event. As a reference, these points have been reported also in the cross section at a arbitrary depth of 20 km to do not overlap with instrumental seismicity (see text for details). Boxes containing dates are the macro-seismic epicentres of the historical earthquakes.

Figure 2. (a) One-dimensional P-wave velocity models. Black line for Bagh et al., (2007), grey line for Chiarabba et al., (2009) and red line for the gradient model used in this study. Wadati diagram of the V_P/V_S ratio respectively for the foreshock (2b) and aftershock sequence (2c).

Figure 3. Seismic stations distribution: grey squares indicate the RSNC stations, while triangles and diamonds show the location of the INGV and LGIT mobile networks, respectively.

Figure 4. Location parameters for the foreshock dataset.

Figure 5. Location parameters for the aftershock dataset.

Figure 6. Spatio-temporal evolution of the seismicity in the epicentral area in 2009.

Figure 7: The grey line represents the cumulative number of events versus time (grey curve) for the whole 2009. While the points are the event magnitude distribution versus time.

Figure 8. Number of Events versus depth for the foreshocks (red line), aftershocks (black line) and events larger than M_W 4.0 (purple).

Figure 9. Map view of seismicity distribution: red points for foreshocks and black points for aftershocks. The locations (stars) of the larger events (M_W>3.5) of the sequence are reported colour coded by their size. Dark brown lines represent the Quaternary mapped normal faults (EMERGEO Working Group, 2010 and reference therein). The N45E-trending thin lines are the traces of the 14 vertical cross sections of Figure 10. In yellow we trace also the main surface breakages as mapped by the EMERGEO Working Group (2010).

Figure 10. Vertical cross sections for the Southern (10a), L'Aquila (10b), Campotosto (10c) and Cittareale (10d) areas. We report with the brown points located at 0 km of elevation the intersection between mapped fault and cross section traces. While yellow points indicate the intersections between the surface breakage and section traces. We report also the names of the most significative faults and geographic locations. Note that in the majority of the cross sections of Figure 10a we project also the seismicity of cross section number 20 where it is easy to appreciate the SDP-MS fault geometry.

Figure 11. Location (this study) and focal mechanisms solution (Scognamiglio et al., in press) of the M_W>3.5 events (see also Table 2).

Table 2. Location (this study), focal mechanisms and source parameters (Scognamiglio et al., submitted) for the events with M_W>3.5.

Y M D	H.M	Lat	Lon	D	Mw	Str_1	Dip_1	R_1	Str_2	Dip_2	R_2	Moment
20090330	13.38	42.33	13.3795	9.2	4	117	62	-129	357	47	-40	1.06 e22
20090330	13.43	42.3353	13.3862	11.58	3.46	149	53	-86	323	37	-95	1.9 e21
20090405	20.48	42.3438	13.3875	9.87	3.88	119	62	-131	0	48	-40	8.15 e21
20090405	22.39	42.3432	13.3952	9.61	3.5	15	61	-35	124	60	-145	2.21 e21
20090406	1.32	42.3502	13.3762	9.28	6.1	139	48	-87	314	42	-94	1.62 e25
20090407	17.47	42.312	13.472	14.11	5.4	338	73	-58	93	36	-151	1.42 e 24
20090409	0.53	42.507	13.3687	10.91	5.21	322	46	-95	149	45	-85	8.25 e23
20090406	2.37	42.37	13.3415	9	4.85	140	53	-103	340	39	-74	2.34 e23
20090406	23.15	42.4735	13.4008	9.22	4.98	154	57	-80	316	34	-106	3.69 e 23
20090407	9.26	42.3412	13.4	7.48	4.93	143	63	-91	326	27	-88	3.06 e23
20090409	19.38	42.5217	13.3715	7.16	4.96	137	48	-86	311	42	-95	3.46 e23
20090413	21.14	42.5145	13.39	7.72	4.83	138	49	-96	327	42	-83	2.2 e23
20090406	3.56	42.3397	13.382	7.96	4.3	143	55	-94	330	35	-84	3.35 e22
20090406	7.17	42.3662	13.3893	7.94	4.1	118	59	-108	329	36	-64	1.6 e22
20090406	16.38	42.3683	13.3402	8.97	4.25	138	51	-106	342	42	-72	2.92 e22
20090407	21.34	42.37	13.3693	7.04	4.29	310	46	-83	120	44	-97	3.35 e22
20090409	3.14	42.3428	13.4487	14.27	4.2	156	87	60	62	30	175	2.48 e22
20090409	4.32	42.4537	13.4502	7.01	4.11	122	54	-124	351	48	-52	1.81 e22
20090423	15.14	42.2545	13.496	6.43	4	126	56	-88	302	34	-93	1.19 e22
20090622	2058	42.452	13.3557	11.1	4.4	316	88	-76	55	14	-170	4.36 e 22
20090712	838	42.3348	13.3895	9.23	4.2	138	61	-101	341	31	-71	2.17 e22
20090423	21.49	42.246	13.5013	6.53	4.18	133	53	-96	322	38	-82	2.3 e22
20090406	4.47	42.3623	13.3455	6.29	3.8	129	59	-123	1	44	-48	6.7 e21
20090406	1012	42.317	13.384	9	3.6	144	51	-100	339	40	-78	3.43 e21
20090406	21.56	42.3888	13.34	6.85	3.7	140	46	-104	340	46	-76	4.06 e21
20090406	22.47	42.3448	13.3102	10.52	3.6	104	58	-120	332	42	-51	3.39 e21
20090407	21.39	42.3637	13.367	8.49	3.6	127	64	-123	3	41	-42	3.29 e21
20090408	3.00	42.3018	13.4747	6.14	3.6	131	73	-115	8	30	-36	3.47 e21
20090408	4.27	42.3042	13.4782	6.37	3.8	124	71	-113	355	29	-43	6.26 e21
20090408	22.56	42.509	13.3735	7.96	3.8	329	47	-67	117	47	-113	7.30 e21
20090409	4.43	42.5103	13.3807	7.96	3.7	136	55	-86	308	35	-96	4.03 e21
20090409	13.19	42.3435	13.2695	9.75	3.8	115	56	-108	325	38	-66	6.30 e21
20090409	22.40	42.4892	13.314	11.03	3.6	316	90	-92	220	2	-6	3.31 e21
20090410	3.22	42.471	13.4302	7.28	3.7	134	47	-88	311	43	-92	4.11 e21
20090413	13.36	42.4458	13.4583	7.39	3.6	116	69	-152	15	64	-24	2.94 e21
20090413	19.09	42.3645	13.3645	9.03	3.7	126	63	-122	0	41	-44	4.09 e21
20090414	1356	42.549	13.3253	8.37	3.8	332	46	-95	160	45	-85	6.21e21
20090414	20.17	42.5445	13.3035	8.55	3.74	137	47	-107	341	45	-72	5.07 e21
20090414	17.27	42.5445	13.3035	8.55	3.6	123	50	-118	343	47	-61	3.45 e21
20090415	22.53	42.529	13.336	8.9	3.8	132	49	-100	328	42	-78	6.91 e21
20090416	17.49	42.5483	13.295	9.07	3.7	335	60	-87	150	30	-95	4.80 e21
20090418	9.05	42.4452	13.3577	11.46	3.7	311	66	-110	172	31	-53	5.17 e21
20090421	1544	42.3367	13.3818	9.58	3.5	139	54	-107	347	40	-68	2.02 e21
20090430	1301	42.3665	13.3688	8.56	3.5	131	60	-128	8	47	-44	2.31e21
20090501	5.12	42.2937	13.4758	6.76	3.6	142	61	-103	347	32	-68	2.98 e21
20090514	630	42.4917	13.4077	7.59	3.4	154	48	-86	328	42	-94	177 e21
20090530	2.55	42.359	13.3553	9.62	3.6	139	56	-106	345	37	-68	2.73 e21
20090623	0.41	42.4498	13.3642	10.9	3.7	315	85	-101	201	12	-24	4.47 e21
20090625	2100	42.5715	13.2037	8	3.5	143	52	-76	301	40	-107	2.07 e21
20090703	1103	42.399	13.3892	4.77	3.7	289	46	-91	111	44	-88	5.09 e21
20090712	22.14	42.3432	13.3882	9.08	3.7	116	60	-115	339	39	-54	3.73 e21
20090731	11.05	42.2565	13.5007	6.14	3.9	145	60	-94	333	30	-83	8.23 e21
20090924	1614	42.4652	13.35	13.23	3.9	178	49	-91	359	41	-89	9.29 e21
20091020	507	42.3948	13.2385	9.79	3.5	20	81	-23	114	67	-171	2.17 e21

References.

Aldersons F., R. Di Stefano, L. Chiaraluce, D. Piccinini and L. Valoroso (2009), Automatic detection and P- and S-wave picking algorithm: an application to the 2009 L'Aquila (Central Italy) earthquake sequence. AGU Fall Meeting, San Francisco December 14-18.

Antonioli A., Simone Atzori, Claudio Chiarabba, Lauro Chiaraluce, Massimo Cocco (2009), Stress evolution during the April 2009 L'Aquila Seismic Poster sequence (central Italy). AGU Fall Meeting, San Francisco December 14-18.

Anzidei, M., E. Boschi, V. Cannelli, R. Devoti, A. Esposito, A. Galvani, D. Melini, G. Pietrantonio, F. Riguzzi, V. Sepe, and E. Serpelloni (2009), Coseismic deformation of the destructive April 6, 2009 L'Aquila earthquake (central Italy) from GPS data, Geophys. Res. Lett., 36, L17307, doi:10.1029/2009GL039145.

Atzori, S., I. Hunstad, M. Chini, S. Salvi, C. Tolomei, C. Bignami, S. Stramondo, E. Trasatti, A. Antonioli and E. Boschi (2009), Finite fault inversion of DInSAR coseismic displacement of the 2009 L'Aquila earthquake (central Italy). Geophys. Res. Lett., 36, L15305, doi:10.1029/2009GL039293.

Bagnaia, R., A. D'Epifanio, and S. Sylos Labini (1992), Aquila and subaequan basins: An example of Quaternary evolution in central Apennines, Italy, Quat. Nova, II, 187– 209.

Bagh S., L. Chiaraluce, P. De Gori, M. Moretti, A. Govoni, C. Chiarabba, P. Di Bartolomeo and M. Romanelli (2007), Background seismicity in the Central Apennines of Italy: The Abruzzo region case study, Tectonophysics 444 (2007) 80–92.

Barchi, M., F. Galadini, G. Lavecchia, P. Messina, A. M. Michetti, L. Peruzza, A. Pizzi, E. Tondi, and E. Vittori (2000), Sintesi delle conoscenze sulle faglie attive in Italia centrale: Parametrizzazione ai fini della caratterizzazione della pericolosita` sismica, report for CNR, Gruppo Naz. per la Difesa dai Terr., Rome.

Boncio, P., G. Lavecchia, and B. Pace (2004), Defining a model of 3D seismogenic sources for Seismic Hazard Assessment applications: The case of central Apennines (Italy), J. Seismol., 8, 407– 425, doi:10.1023/B:JOSE.0000038449.78801.05.

Boncio, P., Lavecchia, G., Milana, G., Rozzi, B., (2004), Improving the knowledge on the seismogenesis of the Amatrice–Campotosto area (central Italy) through an integrated analysis of minor earthquake sequences and structural data. Ann. Geophys. 47, 1723–1742.

Boncio P., A. Pizzi, F. Brozzetti, G. Pomposo, G. Lavecchia, D. Di Naccio, and F. Ferrarini (2010), Geophys. Res. Lett., 37, L06308, doi:10.1029/2010GL042807.

Calamita, F., Viandante, M.G., Hegarty, K. (2004), Pliocene-Quaternary burial/exhumation paths of the central Apennines (Italy): Implications for the definition of the deep structure of the belt, Boll. Soc. Geol. Ital., 123, 503–512.

Cavinato, G.P., De Cellis, P.G., (1999), Extensional basins in the tectonically bimodal central Apennines fold-thrust belt, Italy: response to corner flow above a subduction slab in retrograde motion. Geology 27, 955–958.

Çelebi M., P. Bazzurro, L. Chiaraluce, P. Clemente, L. Decanini, A. DedeSortis, W. Ellsworth, A. Gorini, E. Kalkan, S. Marcucci, G. Milana, F. Mollaioli, M. Olivieri, R. Paolucci, D. Rinaldis, A. Rovelli, F. Sabetta and C. Stephens. Recorded Motions of the Mw 6.3 April 6, 2009 L'Aquila (Italy) Earthquake and Implications for Building Structural Damage: Overview (2010), Eartquake Spectra, 26 (2010), 3, 651-684.

Chiarabba, C., Jovane, L., DiStefano, R., (2005), A new view of Italian seismicity using 20 years of instrumental recordings. Tectonophysics 395, 251–268.

Chiarabba, C., A. Amato, M. Anselmi, P. Baccheschi, I. Bianchi, M. Cattaneo, G. Cecere, L. Chiaraluce, M. G. Ciaccio, P. De Gori, G. De Luca, M. Di Bona, R. Di Stefano, L. Faenza, A. Govoni, L. Improta, F. P. Lucente, A. Marchetti, L. Margheriti, F. Mele, A. Michelini, G. Monachesi, M. Moretti, M. Pastori, N. Piana Agostinetti, D. Piccinini, P. Roselli, D. Seccia, and L. Valoroso (2009), The 2009 L'Aquila (central Italy) MW6.3 earthquake: Main shock and aftershocks. Geophys. Res. Lett., 36, L18308, doi:10.1029/2009GL039627.

Chiaraluce, L., Ellsworth, W.L., Chiarabba, C., Cocco, M., (2003), Imaging the complexity of an active normal fault system: the 1997 Colfiorito (central Italy) case study. J. Geophys. Res. 108 (B6), 2294. doi:10.1029/2002JB002166.

Chiaraluce, L., M. Barchi, C. Collettini, F. Mirabella, and S. Pucci (2005), Connecting seismically active normal faults with Quaternary geological structures in a complex extensional environment: The Colfiorito 1997 case history (northern Apennines, Italy), Tectonics, 24, TC1002, doi:10.1029/2004TC001627.

Chiaraluce, L., C. Chiarabba, C. Collettini, D. Piccinini, and M. Cocco (2007), Architecture and mechanics of an active low-angle normal fault: Alto Tiberina Fault, northern Apennines, Italy, J. Geophys. Res., 112, B10310, doi:10.1029/2007JB005015.

Chiaraluce L., L. Valoroso, M. Anselmi, S. Bagh and C. Chiarabba (2009), A decade of passive seismic monitoring experiments with local networks in four Italian regions, Tectonophysics 476 85–98.

Ciaccio M.G., Palombo B., Bernardi F. (2009), The main seismic sequences occurred between 1981-2008 in the L'Aquila region. FIST, 09-11 September 2009, GEOITALIA: VII Forum Italiano di Scienze della Terra, Rimini.

Cirella, C., A. Piatanesi, M. Cocco, E. Tinti, L. Scognamiglio, A. Michelini, A. Lomax, and E. Boschi (2009), Rupture history of the 2009 L'Aquila (Italy) earthquake from non-linear joint inversion of strong motion and GPS data. Geophys. Res. Lett., 36, L19304, doi:10.1029/2009GL039795.

D'Agostino, N., Giuliani, R., Mattone, M., Bonci, L., (2001), Active crustal extension in the central Apennines (Italy) inferred from GPS measurements in the interval 1994–1999. Geophys. Res. Lett. 28, 2121–2124.

D'Agostino, N., A. Avallone, D. Cheloni, E. D'Anastasio, S. Mantenuto, and G. Selvaggi (2008), Active tectonics of the Adriatic region from GPS and earthquake slip vectors, J. Geophys. Res., 113, B12413, doi:10.1029/2008JB005860.

De Luca, G., Scarpa, R., Filippi, L., Gorini, A., Marcucci, S., Marsan, P., Milana, G., Zambonelli, E., (2000), A detailed analysis of two seismic sequences in Abruzzo, central Apennines, Italy. J. Seismol. 4, 1–21.

Deschamps, A., Iannaccone, G. and Scarpa, R., 1984, The Umbrian earthquake (Italy) of 19 September 1979, Ann. Geophys. 2, 1, 29–36.

Di Luccio, F., G. Ventura, R. Di Giovambattista, A. Piscini, and F. R. Cinti (2010), Normal faults and thrusts reactivated by deep fluids: The 6 April 2009 Mw 6.3 L'Aquila earthquake, central Italy, J. Geophys. Res., 115, B06315, doi:10.1029/2009JB007190.

Di Stefano R., C. Chiarabba, L. Chiaraluce, M. Cocco, P. De Gori, D. Piccinini and L. Valoroso, Fault properties heterogeneity affecting the rupture evolution of the 2009 (Mw 6.1) L'Aquila earthquake (Central Italy): insights from seismic tomography. Submitted to GRL.

Ellsworth W. and L. Chiaraluce (2009), Supershear During Nucleation of the 2009 M 6.3 L'Aquila, Italy Earthquake. AGU Fall Meeting, San Francisco December 14-18.

EMERGEO Working Group (2010), Evidence for surface rupture associated with the Mw 6.3 L'Aquila earthquake sequence of April 2009 (central Italy), Terra Nova, 22, 43–51, 2010 doi: 10.1111/j.1365-3121.2009.00915.x.

Falcucci E., S. Gori, E. Peronace, G. Fubelli, M. Moro, M. Saroli, B. Ciaccio, P. Messina, G. Naso, G. Scardia, A. Sposato, M. Voltaggio, P. Galli and F. Galadini (2009), The Paganica Fault and Surface Coseismic Ruptures Caused by the 6 April 2009 Earthquake (L'Aquila, Central Italy). Seismological Research Letters, vol. 80, n. 6.

Galadini, F., Galli, P., (2000). Active tectonics in the central Apennines (Italy) — input data for seismic hazard assessment. Nat. Hazards 22, 225–270.

Galadini, F., Galli, P., (2003), Paleoseismology of silent faults in the Central Apennines (Italy): the Mt. Vettore and Laga Mts. Faults. Ann. Geophys. 5, 815–836.

Hunstad, I., Selvaggi, G., D'Agostino, N., Englaand, P., Clarke, P., Pierozzi, M., (2003), Geodetic strain in peninsular Italy between 1875 and 2001. Geophys. Res. Lett. 30 (4).

Kissling, E., W.L. Ellsworth, D. Eberhart-Phillips, and U. Kradolfer (1994), Initial reference models in local earthquake tomography, J. Geophys. Res., 99, 19635-19646, 1994.

Kradolfer, U., 1989, Seismische Tomografie in der Schweiz mittels lokaler Erdbeben, PhD Thesis, Eidgenössischen Tech. Hoch., Zürich, Switzerland pp. 109.

Lahr, J.C., 1989. HYPOELLIPSE/version 2.00: a computer program for determining local earthquakes hypocentral parameters, magnitude and first motion pattern. U.S. Geol. Surv Open-File Rep., vol. 89-116, p. 92.

Lavecchia, G., Brozzetti, F., Barchi, M., Keller, J., Meinichetti, M., (1994), Seismotectonic zoning in east–central Italy deduced from the analysis of the Neogene to present deformations and related stress fields. Geol. Soc. Amer. Bull. 106, 1107–1120.

Lee, W.H.K., Lahr, J.C., (1975). HYPO71: a computer program for determining hypocenter, magnitude and first motion pattern of local earthquakes. U. S. Geol. Surv Open-File Rep., vol. 75-311, pp. 1–116.

Lucente F. P., De Gori P., Margheriti L., Piccinini D., Di Bona M., Chiarabba C. And N. Piana Agostinetti (2009). The preparatory phase of the April 6th 2009, Mw 6.3, L'Aquila earthquake: Seismological observations, AGU Fall Meeting, San Francisco December 14-18.

Mariucci, M.T., Amato, A., Montone, P., (1999), Recent tectonic evolution and present day stress in the Northern Apennines (Italy). Tectonics 18 (1), 108–118.

Mazzoli, S., Pierantoni, P.P, Borraccini, F., Paltrinieri, W., Deiana, G. (2005), Geometry, segmentation pattern and displacement variations along a major Apennine thrust zone, central Italy, Journal of Structural Geology, 27, 11, pp. 1940-1953

Mendoza, C., and S. H. Hartzell, Aftershock pattern and mainshock faulting, Bull. Seismol. Soc. Am., 78, 1438– 1449, 1988.

Montone, P., Mariucci, M.T., Pondrelli, S., Amato, A., (2004), An improved stress map for Italy and surrounding regions (central Mediterranean). J. Geophys. Res. 109, B10410. doi:10.1029/ 2003JB002703.

Omori, F., 1895. On the aftershocks of earthquakes. J. College Sci. Imper. Univ. Tokyo 7, 111–200.

Pace, B., Boncio, P., Lavecchia, G., (2002), The 1984 Abruzzo earthquake (Italy): an example of seismogenic process controlled by interaction between differently oriented synkinematic faults. Tectonophysics 350, 237–254.

Patacca, E., Scandone, P., Di Luzio, E., Cabinato, G.P., Parlotto, M. (2008), Structural architecture of the central Apennines: interpretation of the CROP11 seismic profile from the Adriatic coast to the orographic divide, Tectonics, 27, TC30006.

Pino, N. A., and F. Di Luccio (2009), Source complexity of the 6 April 2009 L'Aquila (central Italy) earthquake and its strongest aftershock revealed by elementary seismological analysis, Geophys. Res. Lett., 36, L23305, doi:10.1029/2009GL041331.

Roberts, G.P., Michetti, A., (2004), Spatial and temporal variations in growth rates along active normal fault systems; an example from the Lazzio–Abruzzo Apennines, central Italy. J. Struct. Geol. 26, 339–376.

Scognamiglio L., E. Tinti, A. Michelini, D. Dreger, A. Cirella, M. Cocco, S. Mazza, and A. Piatanesi, Fast Determination of Moment Tensors and Rupture History: Application to the April 6th 2009, L'Aquila Earthquake. In press on SRL.

Selvaggi, G., Castello, B., Azzara, A., (1997), Spatial distribution of scalar seismic moment release in Italy (1983–1996): seismotectonic implications for the Apennines. Ann. Geofis. 40 (6), 1565–1578.

UNMIG - Italian National Mine Office, 2009, Wells Database available at web site http://unmig.sviluppoeconomico.gov.it/unmig/pozzi/pozzi.asp.

Valoroso L. and L'Aquila 2009 Seismic Network Working Groups (2009), The 2009 L'Aquila Seismic Sequence (Central Apennines): Fault System Geometry and Kinematics. AGU Fall Meeting, San Francisco December 14-18.

Vezzani, L., Ghisetti, F., 1998. Carta geologica dell'Abruzzo, 1:100000, SELCA, Via R. Giuliani, Firenze.

Walters, R. J., J. R. Elliott, N. D'Agostino, P. C. England, I. Hunstad, J. A. Jackson, B. Parsons, R. J. Phillips, and G. Roberts (2009), The 2009 L'Aquila earthquake (central Italy): A source mechanism and implications for seismic hazard, Geophys. Res. Lett., 36, L17312, doi:10.1029/2009GL039337.

Ward, S.N., Valensise, G.R., (1989), Fault parameters and slip distribution of the 1915 Avezzano, Italy, earthquake derived from geodetic observations. Bull. Seismol. Soc. Am. 79, 690–710.

Wilkinson M., Kenneth J. W. McCaffrey, G. Roberts, P. A Cowie, R. Phillips and the L'Aquila post-seismic team (2009), Post-seismic slip on the 6th April 2009 L'Aquila earthquake surface rupture, measured using a terrestrial laser scanner (tripod-mounted lidar). AGU Fall Meeting, San Francisco December 14-18.

Working Group CPTI, (1999), Catalogo parametrico dei terremoti italiani, ING, GNDT, SGA SSN, Bologna.

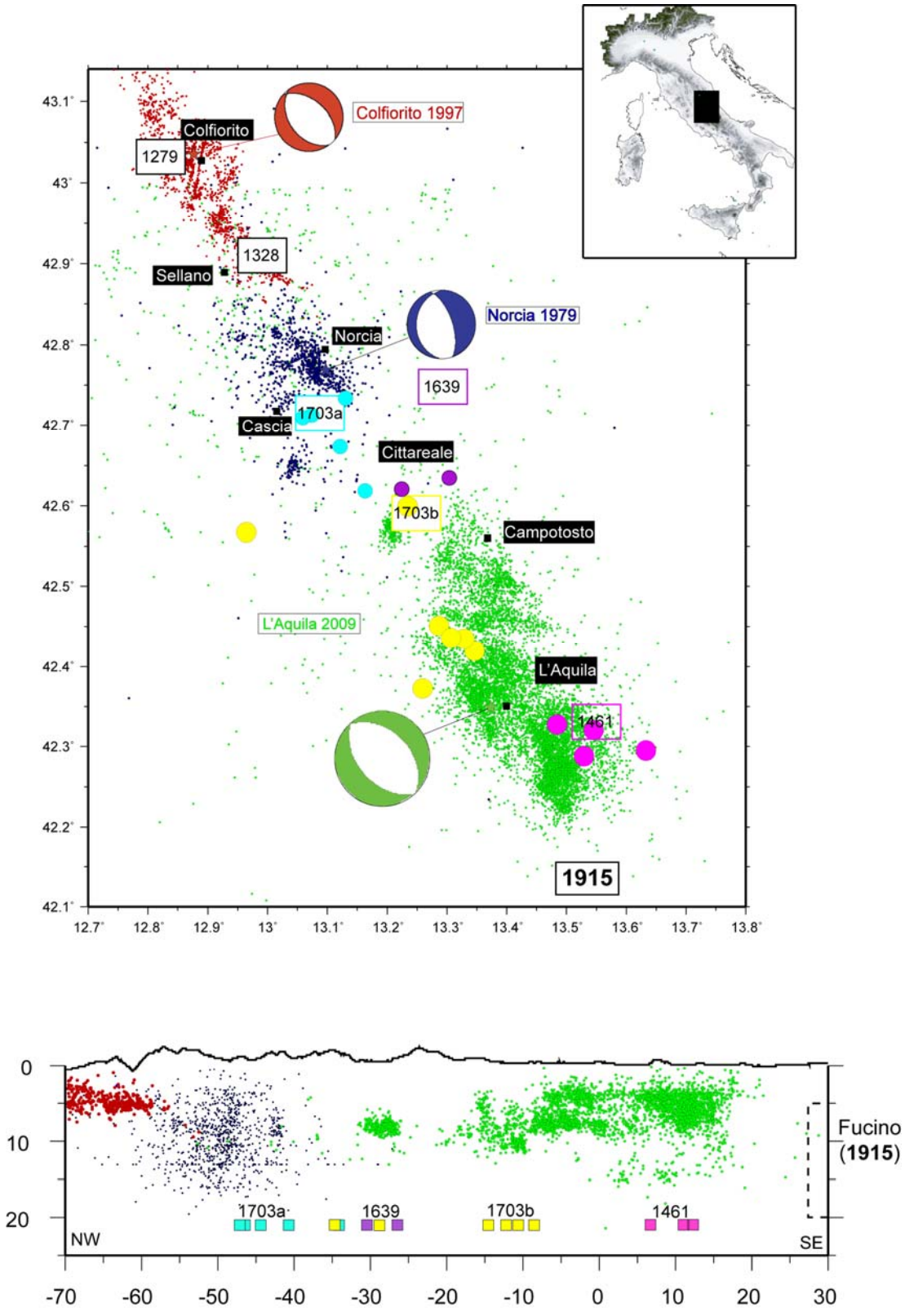
Colfiorito 1997
Colfiorito
1279
1328
Sellano
Norcia 1979
Norcia
1639
1703a
Cascia
Cittareale
1703b
Campotosto
L'Aquila 2009
L'Aquila
1461
1915
43.1°
43°
42.9°
42.8°
42.7°
42.6°
42.5°
42.4°
42.3°
42.2°
42.1°
12.7°
12.8°
12.9°
13°
13.1°
13.2°
13.3°
13.4°
13.5°
13.6°
13.7°
13.8°
0
10
20
1703a
1639
1703b
1461
NW
SE
Fucino
(1915)
-70
-60
-50
-40
-30
-20
-10
0
10
20
30

Figure 1

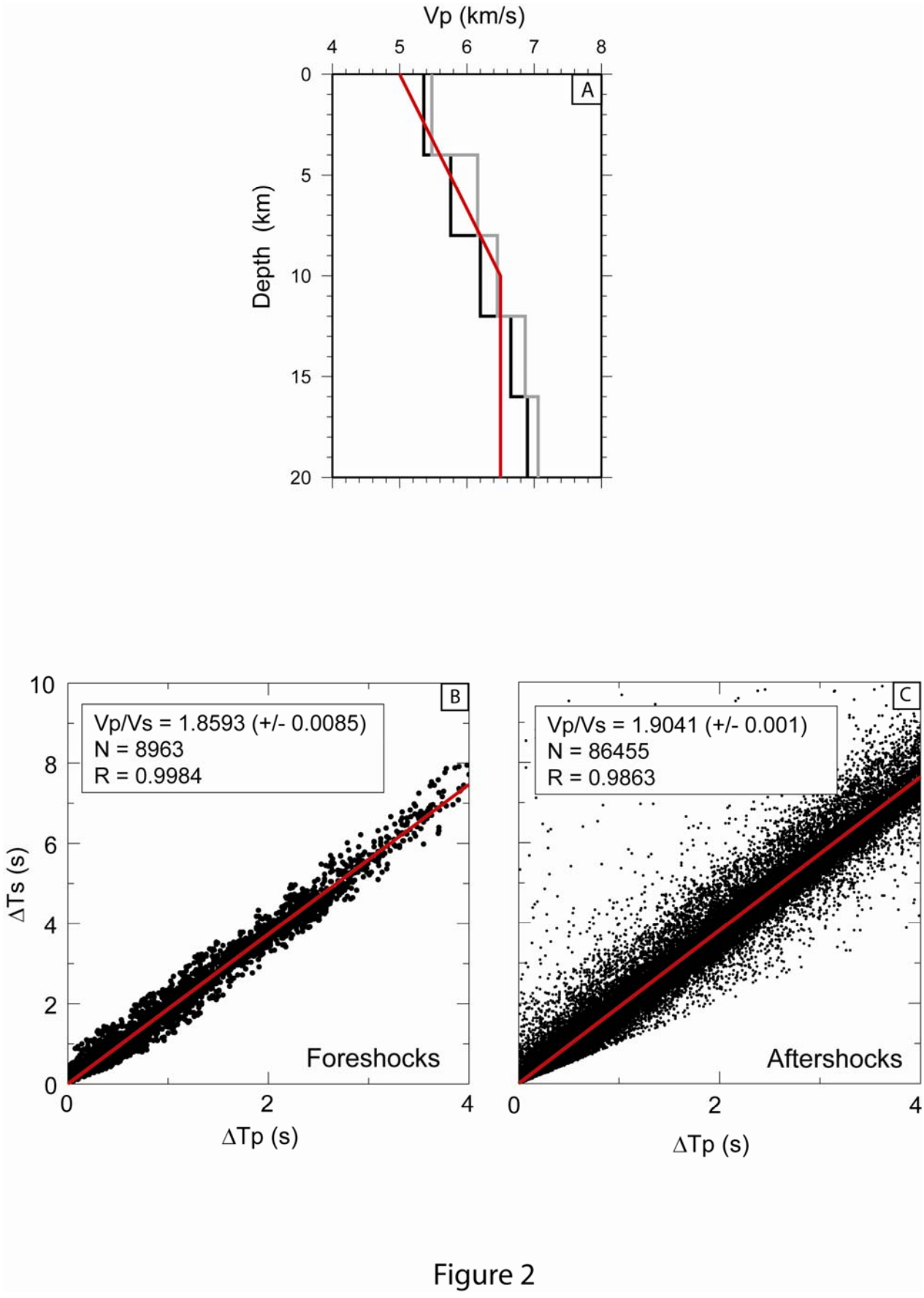
Vp (km/s)
4
5
6
7
8
0
5
10
15
20
Depth (km)
A
B
Vp/Vs = 1.8593 (+/- 0.0085)
N = 8963
R = 0.9984
Foreshocks
ΔTs (s)
ΔTp (s)
C
Vp/Vs = 1.9041 (+/- 0.001)
N = 86455
R = 0.9863
Aftershocks
ΔTp (s)

Figure 2

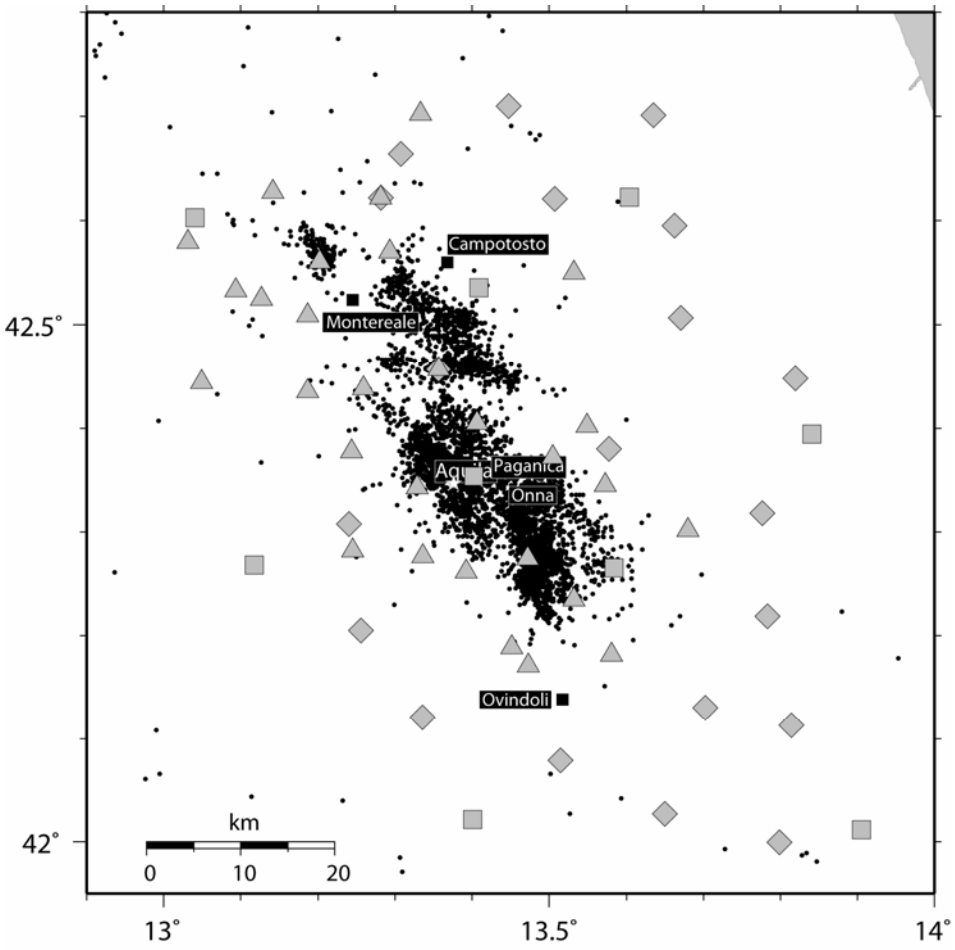
Campotosto
Montereale
Aquila
Paganica
Onna
Ovindoli
km
0
10
20
42.5°
42°
13°
13.5°
14°

Figure 3

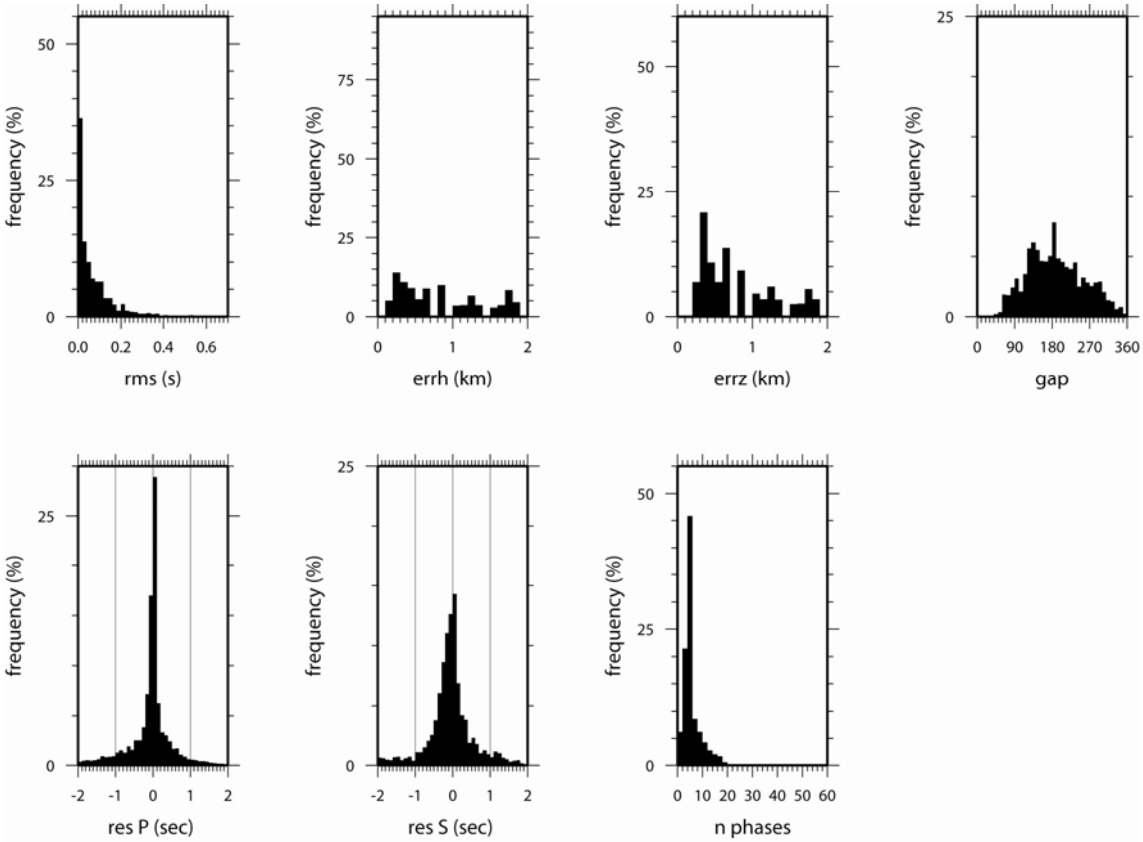

Figure 4

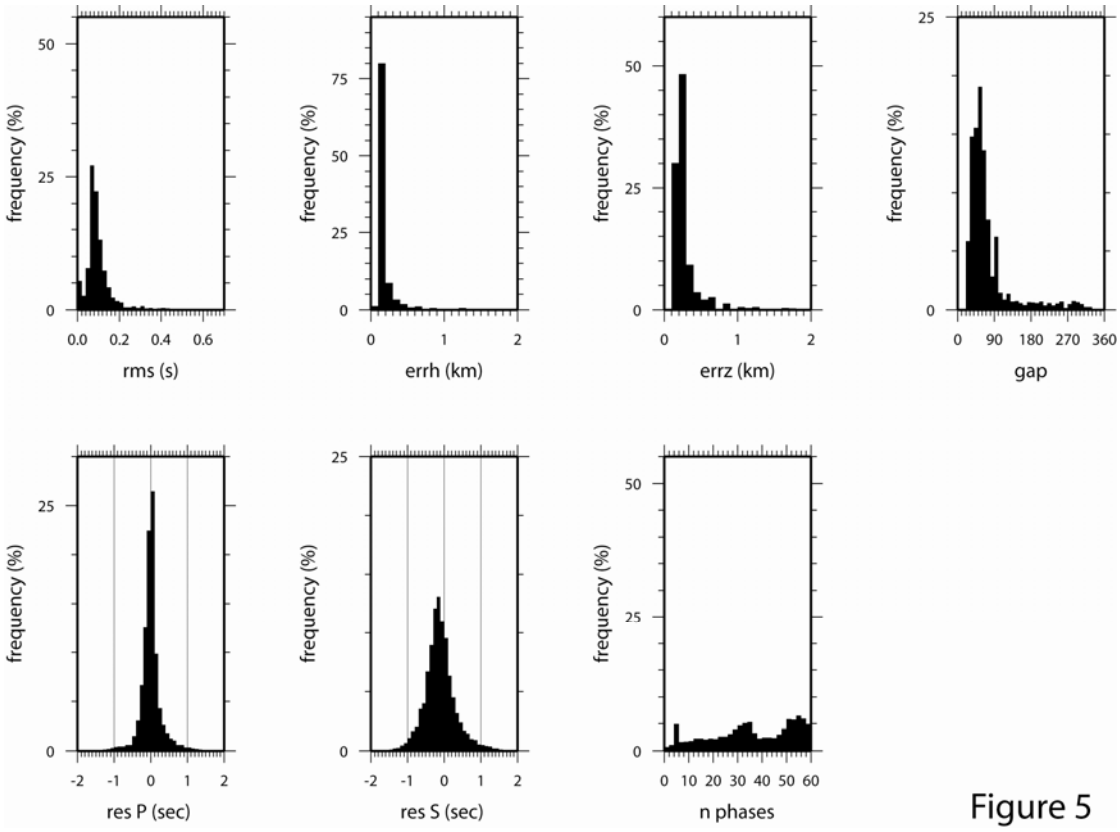

Figure 5

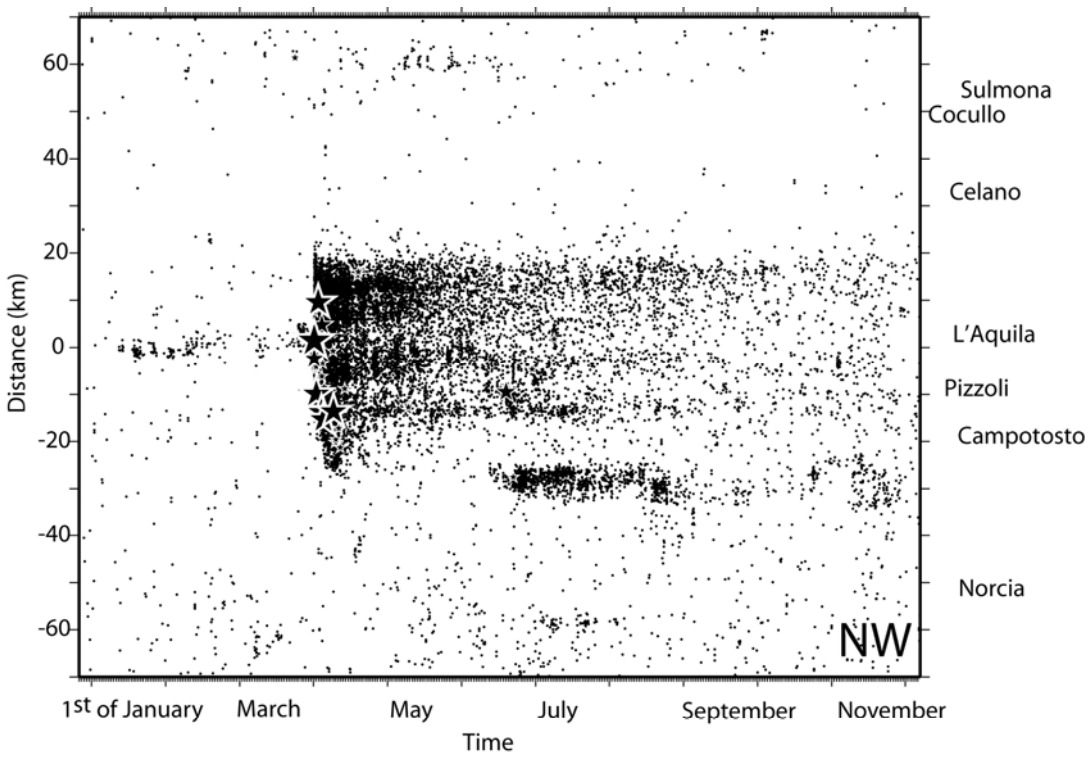
60
40
20
0
-20
-40
-60
Distance (km)
Sulmona
Cocullo
Celano
L'Aquila
Pizzoli
Campotosto
Norcia
NW
1st of January
March
May
July
September
November
Time

Figure 6

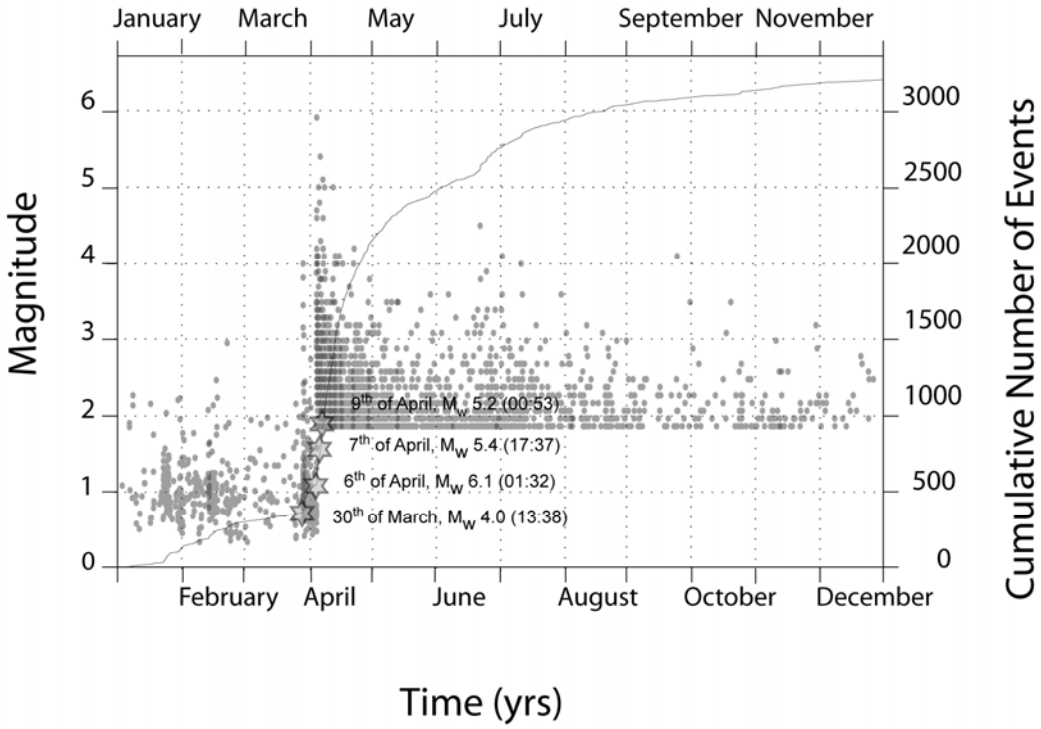
January
March
May
July
September
November
February
April
June
August
October
December
Magnitude
Cumulative Number of Events
Time (yrs)
9th of April, Mw 5.2 (00:53)
7th of April, Mw 5.4 (17:37)
6th of April, Mw 6.1 (01:32)
30th of March, Mw 4.0 (13:38)
0
1
2
3
4
5
6
0
500
1000
1500
2000
2500
3000

Figure 7

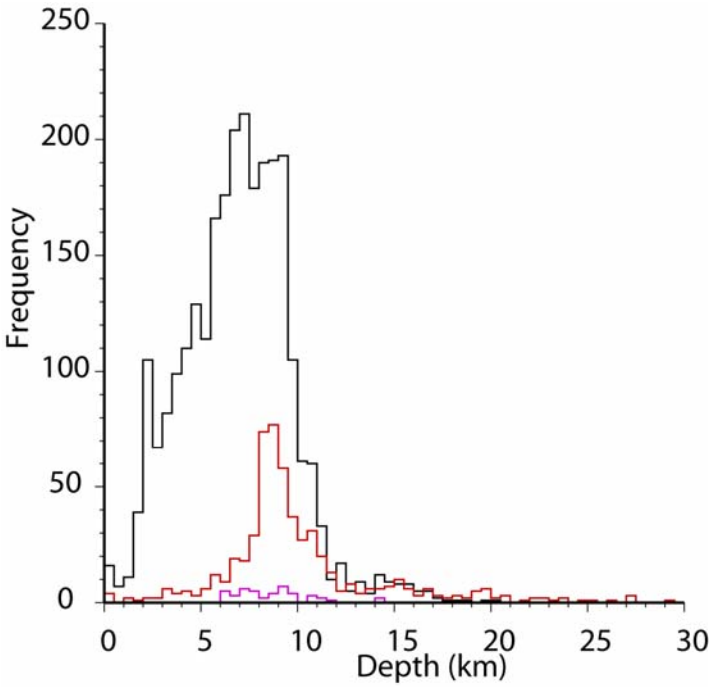

Figure 8

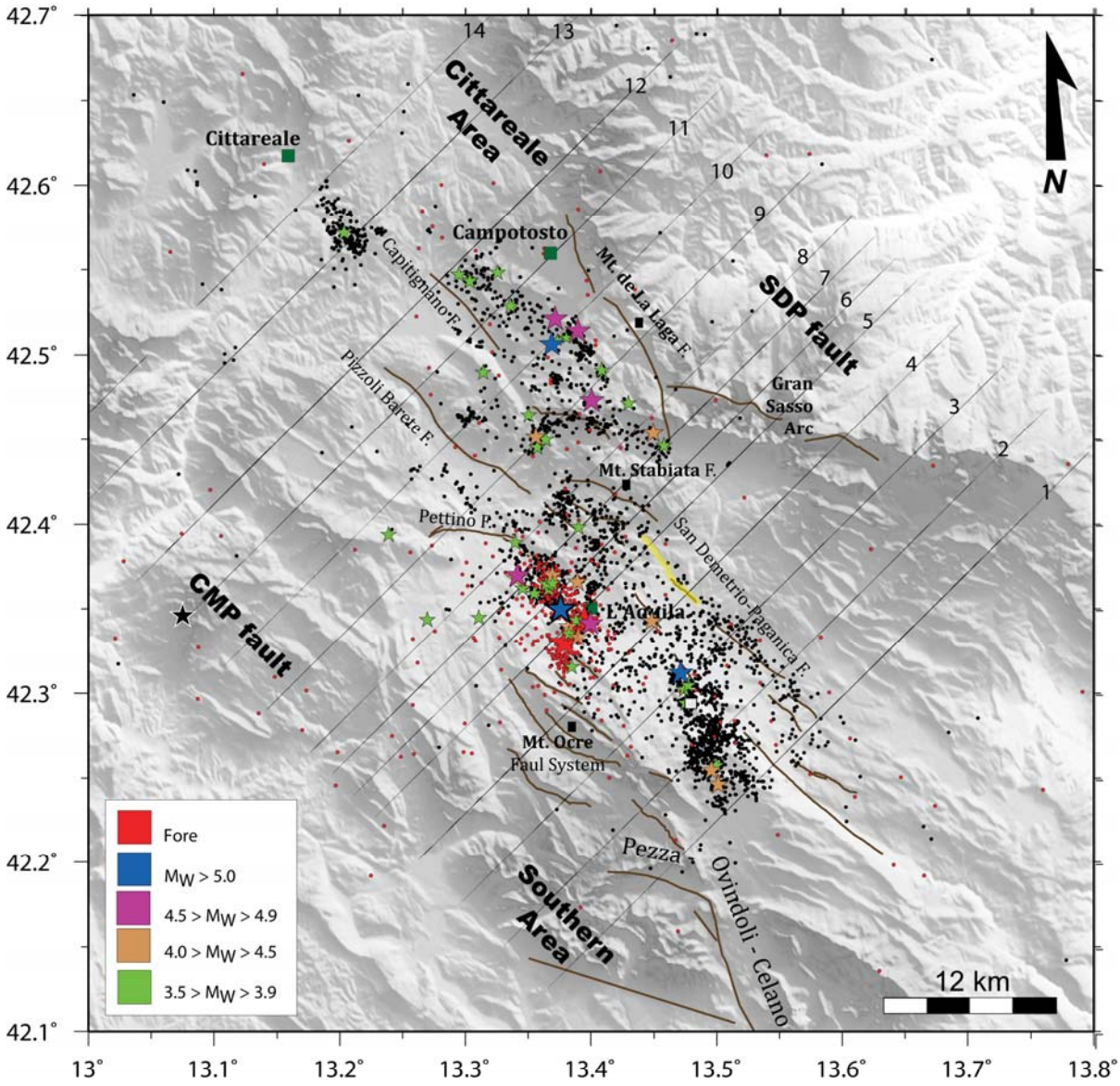
42.7°
42.6°
42.5°
42.4°
42.3°
42.2°
42.1°
13°
13.1°
13.2°
13.3°
13.4°
13.5°
13.6°
13.7°
13.8°
14
13
12
11
10
9
8
7
6
5
4
3
2
1
Cittareale
Area
Cittareale
Campotosto
Capitignano F.
Mt. de La Laga F.
SDP fault
Gran
Sasso
Arc
Pizzoli Barete F.
Mt. Stabiata F.
Pettino P.
San Demetrio-Paganica F.
CMP fault
L'Aquila
Mt. Ocre
Faul System
Pezza
Ovindoli - Celano
Southern
Area
N
12 km
Fore
Mw > 5.0
4.5 > Mw > 4.9
4.0 > Mw > 4.5
3.5 > Mw > 3.9

Figure 9

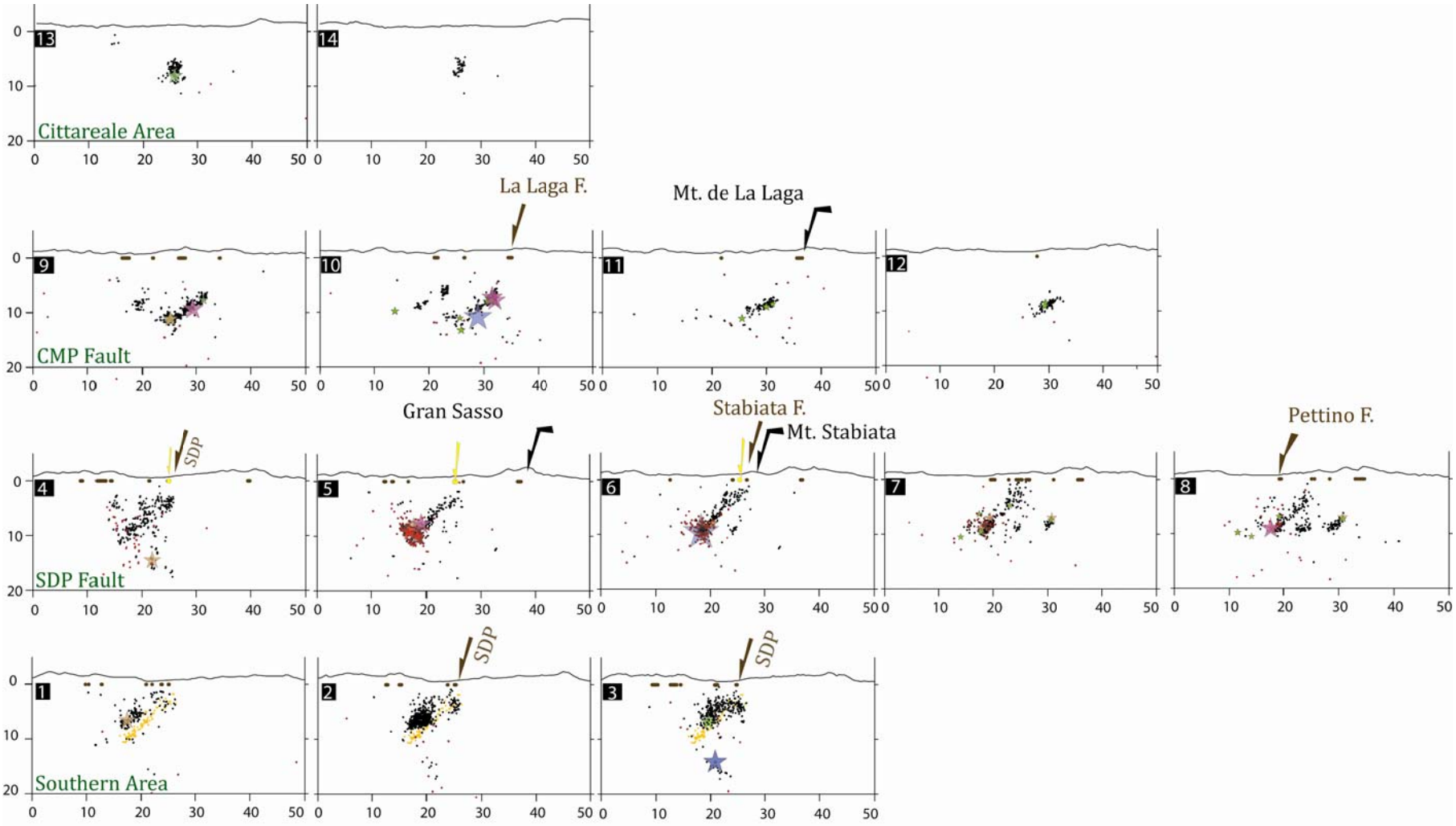
13
14
Cittareale Area
La Laga F.
Mt. de La Laga
9
10
11
12
CMP Fault
Gran Sasso
Stabiata F.
Mt. Stabiata
Pettino F.
SDP
4
5
6
7
8
SDP Fault
SDP
SDP
1
2
3
Southern Area

Figure 10

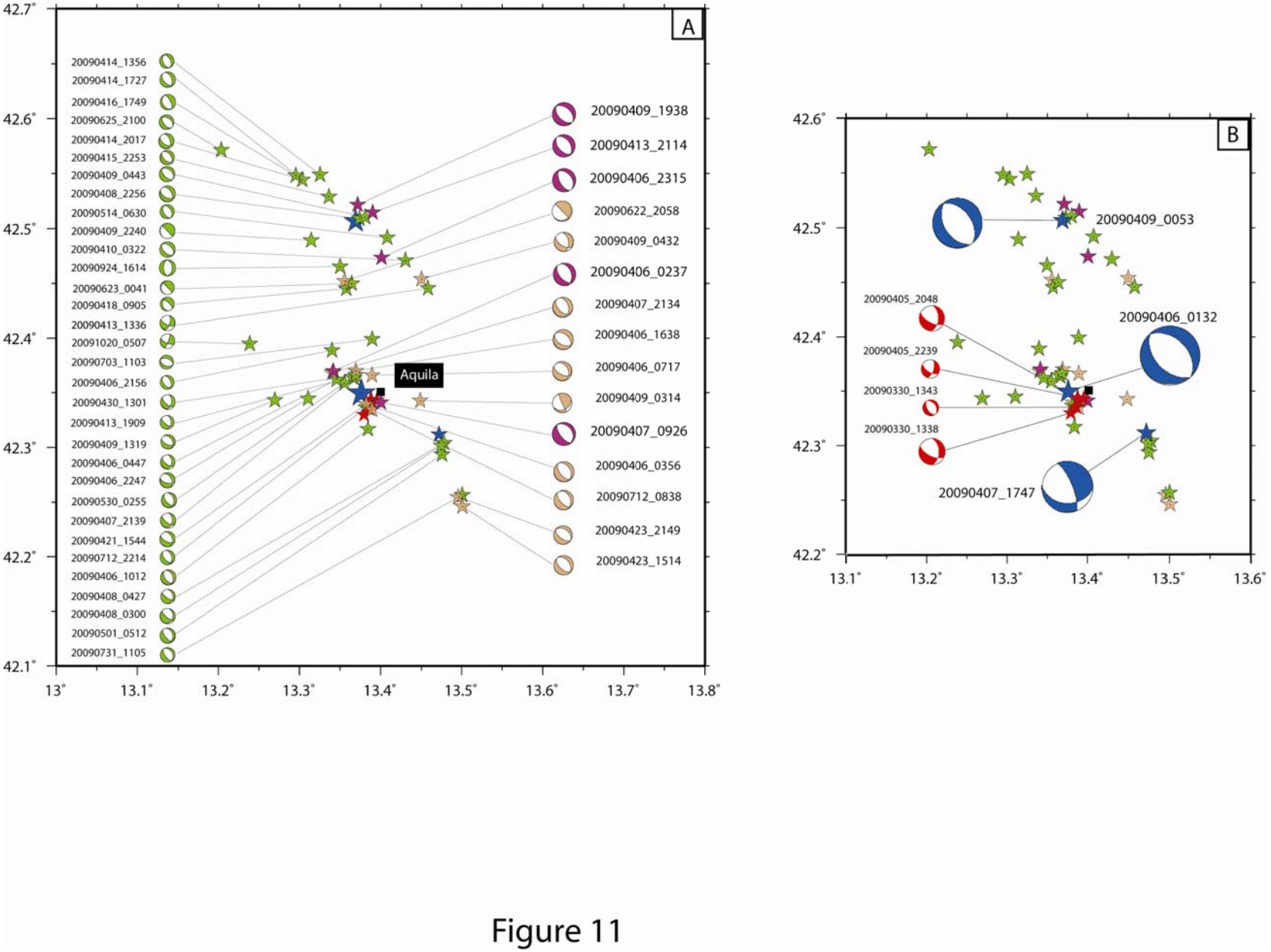
A
B
Aquila
20090414_1356
20090414_1727
20090416_1749
20090625_2100
20090414_2017
20090415_2253
20090409_0443
20090408_2256
20090514_0630
20090409_2240
20090410_0322
20090924_1614
20090623_0041
20090418_0905
20090413_1336
20091020_0507
20090703_1103
20090406_2156
20090430_1301
20090413_1909
20090409_1319
20090406_0447
20090406_2247
20090530_0255
20090407_2139
20090421_1544
20090712_2214
20090406_1012
20090408_0427
20090408_0300
20090501_0512
20090731_1105
20090409_1938
20090413_2114
20090406_2315
20090622_2058
20090409_0432
20090406_0237
20090407_2134
20090406_1638
20090406_0717
20090409_0314
20090407_0926
20090406_0356
20090712_0838
20090423_2149
20090423_1514
20090409_0053
20090405_2048
20090405_2239
20090330_1343
20090330_1338
20090406_0132
20090407_1747
42.7°
42.6°
42.5°
42.4°
42.3°
42.2°
42.1°
13°
13.1°
13.2°
13.3°
13.4°
13.5°
13.6°
13.7°
13.8°

Figure 11